別　刷

計測自動制御学会　論文集

年　　第　　巻　　第　　号

（P.　　～P.　　）

社団法人 計測自動制御学会

[Trans. of the Society of Instrument and Control Engineers Vol. 29, No. 6, 637/646 (1993)]

[計測自動制御学会論文集 Vol. 29, No. 6, 637/646 (1993)]

Multi-Point Compliance Control for Dual-Arm Robots Utilizing Kinematic Redundancy

Achmad JAZIDIE*, Toshio TSUJI*, Mitsuo NAGAMACHI* and Koji ITO**

The present paper proposes a compliance control method utilizing kinematic redundancy of the dual-arm robot. When the dual-arm robot is performing a given task which requires not only the object compliant motion but also the compliant motion of several points on the links of the dual-arm robot, it is needed to control the object compliance and the compliance of those points simultaneously. The method presented here can regulate the compliance of several points on the dual-arm robot as well as the object compliance through regulation of the joint stiffness. The rigid object manipulated by the dual-arm robot can be modeled as a virtual link depending on the size of the object and the contact type between the object and the end-effectors. As a result, the points on the links of the dual-arm robot can be regarded as the virtual point objects grasped by the virtual dual-arm robots, and the compliance control for the virtual objects can be developed as well as the object compliance control. The forward relationship from the joint compliance matrix to the multi-object compliance matrix is formalized, and then the general solution of the inverse problem, that is to specify the joint servo gain of the dual-arm robot to achieve, as close as possible, the desired multi-object compliance is presented. To demonstrate the effectiveness of the proposed method, the simulation experiments are performed.

Key Words: compliance control, kinematic redundancy, dual-arm robot, virtual object

1. Introduction

There are many tasks that require cooperative manipulation by dual-arm robots for industrial manufacturing, ranging from simple handling tasks to more complicated assembly tasks. Also, dual-arm robots may be applied to robotics in unstructured environments such as the space and the ocean where auxiliary equipments are not available[1].

One of the most important features of the dual-arm robot which manipulate a common object is that the arm and the object form a closed kinematic chain. From this feature many interesting problems arise, and a number of interesting works have been appeared. Most of these works have focused on the modeling and analysis of the closed kinematic chain[2)~4)], load or force distribution problem[5)~8)], the dynamic control[9),10)], and actuator redundancy[11)~13)]. However, less attention has been paid to the compliance control for the dual-arm robot.

The compliance control is one of the most effective control methods for manipulators that interact with the environment. The compliance control provides a mechanism for controlling the manipulator's position or force and facilitates a stable behavior during the transition between unconstrained motion and a sudden contact with the environment. Compliance or stiffness of the parallel link structure has been studied by several investigators. For example, Mason and Salisbury[14], Nguyen[15], and Cutkosky and Kao[16] analyzed the grasp compliance for a multifingered robotic hand, and Adli et al.[17] proposed a compliance control method for parallel manipulators utilizing their internal forces.

As is well known, one of the basic characteristics of the dual-arm robot is the redundancy of the joint degrees of freedom. The manipulator with more joint degrees of freedom than the minimum number required for a given task can offer significant advantages: for instance, collision avoidance and avoiding singular configurations of the manipulator in positioning tasks. Although it is widely recognized that the

* Faculty of Engineering, Hiroshima University, Higashi-Hiroshima
** Toyohashi University of Technology, Toyohashi
(Received August 24, 1992)
(Revised January 11, 1993)

TR 0006/93/2906-0637 © 1992 SICE

kinematic redundancy represents a key towards more flexible and sophisticated manipulations, no previous investigations of the compliance control of the parallel link structure have positively utilized kinematic redundancy. Utilizing redundancy, the dual-arm robot can perform subtasks while controlling the object's compliance.

Yokoi et al.[18] proposed the Direct Compliance Control (DCC) method for parallel link arms which utilizes the kinematic redundancy of the robotic system in order to make the joint stiffness matrix become a diagonal matrix. On the other hand, Tsuji et al. proposed a method called the Multi-Point Compliance Control (MPCC) for a single redundant manipulator[19][20]. This method can regulate not only the end-effector compliance but also the compliance of several points on the manipulator's links utilizing kinematic redundancy.

In the present paper, the MPCC for dual-arm robots is developed. When a rigid object is manipulated by the dual-arm robot, we can model the object as a virtual link depending on the size of the object and the contact type between the object and the end-effectors. As a result, a point on the link of the dual-arm robot can be modeled as a virtual point object grasped by a virtual dual-arm robot, and the compliance control for the virtual object can be developed as well as the object compliance control. The method presented here is effective for certain environments where some obstacles impose restrictions on the task space.

First of all, we formalize the kinematic relationships between the joint compliance and the compliance of several virtual objects on the links including the grasped object. We then derive the joint stiffness to achieve the desired multi-object compliance. The dual-arm robot may become over-constrained depending on the contact type and the number of the objects whose compliance we wish to regulate. The method presented here can give the optimal joint stiffness even for the over-constrained cases in the least squared sense. Finally, the effectiveness of the proposed method is shown by computer simulations.

Nomenclature

Σ_w World coordinate system.

Σ_{tr} Transmission coordinate system.

Σ_o Object coordinate system.

Σ_{voi} i-th virtual object coordinate system.

$dX_e \in R^{2l}$ Concatenated end-effector displacements in the end-effector space, respect to the transmission coordinate system, $dX_e = J_o d\theta$.

$dX_{otr} \in R^{l_{c1}+l_{c2}}$ Concatenated end-effector displacements in the transmission space, respect to the transmission coordinate system, $dX_{otr} = HdX_e = HdX_c$.

$dX_c \in R^{2l}$ Concatenated end-effector displacements in the contact-point space, respect to the transmission coordinate system, $dX_c = S^T dX_o$.

$dX_o \in R^l$ Object displacements, respect to the object coordinate system.

$F_e \in R^{2l}$ Concatenated end-effector forces and moments in the end-effector space, respect to the transmission coordinate system, $\tau = J_o^T F_e$.

$F_{otr} \in R^{l_{c1}+l_{c2}}$ Concatenated end-effector forces and moments in the transmission space, respect to the transmission coordinate system, $F_{otr} = HF_e = HF_c$.

$F_c \in R^{2l}$ Concatenated end-effector forces and moments in the contact point space, respect to the transmission coordinate system, $F_c = S^+ F_o$, where the superscript "+" stands for the Moore-Penrose generalized inverse.

$F_o \in R^l$ Object forces and moments, respect to the object coordinate system.

$J_o \in R^{2l \times (m_1+m_2)}$ Concatenated Jacobian matrix of both arms, respect to the transmission coordinate system. J_o = block−diag. $[J_{o1}\ J_{o2}]$, where block−diag. [ ] denotes a block diagonal matrix.

$J_{ok} \in R^{l \times m_k}$ Jacobian matrix of the k-th arm.

$H \in R^{(l_{c1}+l_{c2}) \times 2l}$ Concatenated contact constraint matrix for the object. H = block−diag. $[H_{o1}\ H_{o2}]$.

$H_{ok} \in R^{l_{ck} \times l}$ Contact constraint matrix between the k-th arm and the object.

$S \in R^{l \times 2l}$ Forces and moments transformation matrix for the object, $S = [S_{o1}\ S_{o2}]$.

$S_{ok} \in R^{l \times l}$ Forces and moments transformation matrix corresponding to the k-th arm.

$dX_{vtri} \in R^{2l}$ Concatenated virtual end-effector displacements corresponding to the i-th virtual object, respect to the i-th virtual object coordinate system. Note that $dX_{vei} = dX_{vtri} = dX_{vci} = J_{vi} d\theta$.

$dX_{voi} \in R^{l}$ i-th virtual object displacements, respect to the i-th virtual object coordinate system.

$F_{vtri} \in R^{2l}$ Concatenated virtual end-effector forces and moments corresponding to the i-th virtual object, respect to the i-th virtual object coordinate system. Note that $F_{vei} = F_{vtri} = F_{vci}$.

$F_{voi} \in R^{l}$ i-th virtual object forces and moments, respect to the i-th virtual object coordinate system.

$J_{vi} \in R^{2l \times (m_1+m_2)}$ Concatenated Jacobian matrix corresponding to the i-th virtual object, respect to the i-th virtual object coordinate system, $J_{vi} = \text{block} - \text{diag.}[J_{vi1}\ J_{vi2}]$.

J_{vik} Jacobian matrix of the k-th virtual arm corresponding to the i-th virtual object. Note that the dimension of J_{vik} depending on the location of the virtual object.

$H_{vi} \in R^{2l \times 2l}$ Concatenated contact constraint matrix for the i-th virtual object, $H_{vi} = I_{2l}$.

$S_{vi} \in R^{l \times 2l}$ Forces and moments transformation matrix for the i-th virtual object, $S_{vi} = [I_l\ I_l]$ and $I_l \in R^{l \times l}$ is an $l \times l$ unit matrix.

$dX_{tr} \in R^{2(n-1)l + l_{c1} + l_{c2}}$ Concatenated transmission displacements corresponding to the multi-object, $dX_{tr} = [dX_{vtr1}^T \cdots dX_{vtrn-1}^T\ dX_{otr}]^T$.

$dX \in R^{nl}$ Concatenated multi-object displacements, $dX = [dX_{vo1}^T \cdots dX_{von-1}^T\ dX_o^T]^T$.

$F_{tr} \in R^{2(n-1)l + l_{c1} + l_{c2}}$ Concatenated transmission forces and moments corresponding to the multi-object, $F_{tr} = [F_{vtr1}^T \cdots F_{vtrn-1}^T\ F_{otr}^T]^T$.

$F \in R^{nl}$ Concatenated multi-object forces and moments, $F = [F_{vo1}^T \cdots F_{von-1}^T\ F_o^T]^T$.

$d\theta \in R^{m_1+m_2}$ Concatenated joint displacements of both arms.

$\tau \in R^{m_1+m_2}$ Concatenated joint torques of both arms.

m_k Number of joints of the k-th arm.

n Number of object and virtual objects.

l Dimension of task.

l_{ck} Number of forces/moments which can be transmitted from the k-th end-effector to the object at the k-th contact point.

$C \in R^{nl \times nl}$ Multi-object compliance matrix.

$C^* \in R^{nl \times nl}$ Desired multi-object compliance matrix.

$C_{real} \in R^{nl \times nl}$ Realized multi-object compliance matrix.

C_{tr} Concatenated transmission compliance matrix for all objects, $C_{tr} \in R^{[2(n-1)l + l_{c1} + l_{c2}] \times [2(n-1)l + l_{c1} + l_{c2}]}$.

C_{tr}^* Concatenated desired transmission compliance matrix for all objects, $C_{tr}^* \in R^{[2(n-1)l + l_{c1} + l_{c2}] \times [2(n-1)l + l_{c1} + l_{c2}]}$.

C_j Joint compliance matrix, $C_j \in R^{(m_1+m_2) \times (m_1+m_2)}$.

K_j Joint stiffness matrix, $K_j \in R^{(m_1+m_2) \times (m_1+m_2)}$.

2. Forward Kinematics of Compliance Matrices for Dual-Arm Robots

We consider a dual arm robot manipulating a common object as shown in Fig. 1. The robot is performing a task which requires the object's compliant motion. Since the arms are inserted through the holes of a wall, they may collide with it due to some external force. Then, as shown in Fig. 1, we locate a virtual object on the closest point of each arm to the wall. Using virtual objects, the interaction between the robot and its environment can be considered within the framework of the compliance control method. For example, to avoid any collision, the compliance of the virtual object should be as small (stiff) as possible in the direction of the wall[19].

2.1 Forward Kinematics for Object Compliance

We define a set of Cartesian coordinate system as

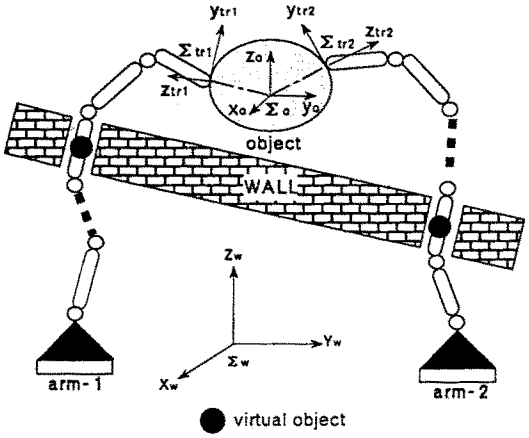

Fig. 1 Dual-arm robot close to the obstacles

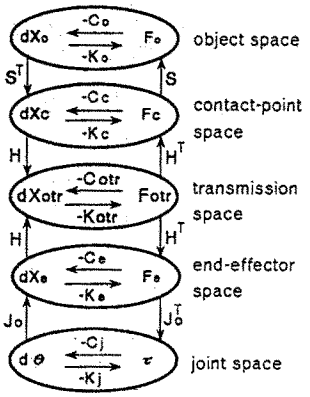

Fig. 2 Force/motion relationships for the object

follows (see **Fig. 1**) : (i) the world coordinate system, Σ_w, is an immobile external coordinate system which acts as a reference frame, (ii) the transmission coordinate system, Σ_{tr}, is a coordinate system located on the object at the contact point where the z axis is normal to the object and the other axes are tangential to the object, and (iii) the object coordinate system, Σ_o, is a mobile coordinate system which changes in accordance to the motion of the object.

Forward force/motion relationships of the dual-arm robot while grasping a common object can be summarized in **Fig. 2**. In the present paper, it is assumed that the contact points between the end-effectors and the object are constant, i. e., there is no slip motion between the end-effectors and the object. For the derivation of the force/motion relationships, see refs. 14), 16) and 21).

The matrix $S=[S_{o1}\ S_{o2}]\in R^{l\times 2l}$, and rank $S=l$, specifies the relationship between the object space and the contact-point space depending on the location of the contact points and the reference point on the object such as the center of mass, where l is the dimension of the object space. The matrix $H=$block $-$diag. $[H_{o1}\ H_{o2}]\in R^{(l_{c1}+l_{c2})\times 2l}$, and rank $H=l_{c1}+l_{c2}$, expresses the filter characteristics which filter out some forces of the end-effectors and transmit other forces to the object depending on the contact type, where block$-$diag. [ ] denotes a block diagonal matrix, and $l_{ck}(k=1, 2)$ denotes the number of forces transmitted from the end-effector of the k-th arm to the object. The matrix $J_o=$block$-$diag. $[J_{o1}\ J_{o2}]$ $\in R^{2l\times(m_1+m_2)}$ is a concatenated Jacobian matrix of both arms relating the joint displacements to the end-effector displacements, represented in the transmission coordinate system, where m_k denotes the number of joints of the k-th arm. If we assume that both arms are not in singular posture, then the rank J_o is equal to $2l$.

Using the force/motion relationships shown in Fig. 2, we can derive the forward kinematic relationships which relate a set of (m_1+m_2) joint coordinates to a set of l object coordinates. The forward kinematic equations of the object are given by:

$$dX_{otr}=G_o dX_o=\beta_o d\theta \tag{1}$$

$$F_o=G_o^T F_{otr} \tag{2}$$

$$\tau=\beta_o^T F_{otr} \tag{3}$$

where

$$G_o=HS^T=\begin{bmatrix}H_{o1}S_{o1}^T\\ H_{o2}S_{o2}^T\end{bmatrix}\in R^{(l_{c1}+l_{c2})\times l} \tag{4}$$

$$\beta_0=HJ_o\in R^{(l_{c1}+l_{c2})\times(m_1+m_2)}$$
$$=\text{block}-\text{diag.}\,[H_{o1}J_{o1}\ H_{o2}J_{o2}] \tag{5}$$

and rank $\beta_o=l_{c1}+l_{c2}$. On the other hand, in order to assure that all forces/moments of the object can be controlled by manipulators, it is assumed that the rank G_o is equal to l.

To derive the forward kinematics for the object compliance, we define the compliance matrices of each space as follows:

Joint Space:

$$d\theta=-C_j\tau \tag{6}$$

$C_j\in R^{(m_1+m_2)\times(m_1+m_2)}$: joint compliance

End-effector Space:

$$dX_e=-C_eF_e \tag{7}$$

$C_e \in R^{2l\times 2l}$: end-effector compliance

Transmission Space:

$$dX_{otr} = -C_{otr}F_{otr} \quad (8)$$

$C_{otr} \in R^{(l_{c1}+l_{c2})\times(l_{c1}+l_{c2})}$: transmission compliance

Contact-Point Space:

$$dX_c = -C_cF_c \quad (9)$$

$C_c \in R^{2l\times 2l}$: contact-point compliance

Object Space:

$$dX_o = -C_oF_o \quad (10)$$

$C_o \in R^{l\times l}$: object compliance

Using (1)~(3) and the compliance matrices defined above, we can obtain the forward kinematic relationship from the joint compliance to the object compliance via the transmission compliance, as given by

$$C_{otr} = G_oC_oG_o^T \quad (11)$$

$$C_{otr} = \beta_oC_j\beta_o^T \quad (12)$$

where G_o and β_o are given in (4) and (5).

2.2 Forward Kinematics for Virtual Object Compliance

To derive the kinematic relationship for the i-th virtual object's compliance, we introduce the virtual dual-arm robot corresponding to the i-th virtual object, as shown in **Fig. 3**. In the virtual dual-arm robot, the grasped object is treated as a virtual link. As a result, for the i-th virtual object, the virtual space with the same kind of definition of compliance matrices as (6)~(10) is given as **Fig. 4**.

Furthermore, for the i-th virtual object, we use two kinds of coordinate systems: (i) the world coordinate system, Σ_w, and (ii) the virtual object coordinate system, Σ_{voi}.

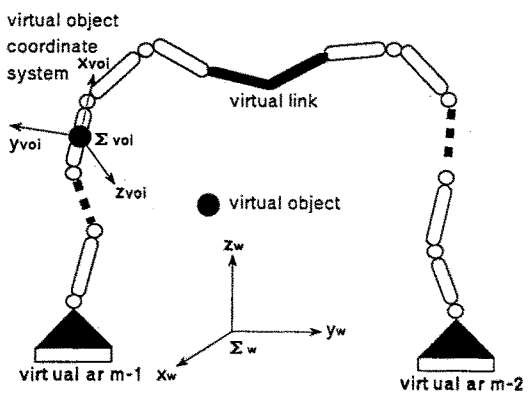

Fig. 3 Virtual dual-arm robot for the i-th virtual object

For the virtual object, the contact type between the virtual end-effectors and the virtual object is always like rigid grasping, i.e., all forces of the virtual end-effectors can be transmitted to the virtual object. Moreover, the virtual object is always like a point object. As a result, we have

$$S_{vi} = [I_l I_l] \in R^{l\times 2l} \quad (13)$$

$$H_{vi} = I_{2l} \in R^{2l\times 2l} \quad (14)$$

where the rank S_{vi} is equal to l and the rank H_{vi} is equal to $2l$. Here, subscript i stands for the i-th virtual object and I_l is an $l\times l$ unit matrix.

The forward kinematic equations of the i-th virtual object are given by

$$dX_{vtri} = G_{vi}dX_{voi} = \beta_{vi}d\theta \quad (15)$$

$$F_{voi} = G_{vi}^TF_{vtri} \quad (16)$$

$$\tau = \beta_{vi}^TF_{vtri} \quad (17)$$

where

$$G_{vi} = H_{vi}S_{vi}^T = \begin{bmatrix} I_l \\ I_l \end{bmatrix} \in R^{2l\times l} \quad (18)$$

$$\beta_{vi} = H_{vi}J_{vi} = J_{vi} \in R^{2l\times(m_1+m_2)} \quad (19)$$

and J_{vi}=block−diag.$[J_{vi1}\ J_{vi2}]$ is the concatenated Jacobian matrix of both virtual arms corresponding to the i-th virtual object, relating the joint displacements to the virtual end-effector displacements, and represented in the i-th virtual object coordinate system.

Here, the rank of $G_{vi}=l$, and the rank of $\beta_{vi}\leq 2l$ depending on the contact type and location of virtual objects. For example, if a virtual object is located on the link of arm-1, then J_{vi} is given by

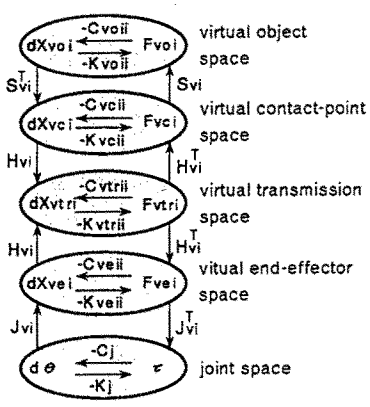

Fig. 4 Force/motion relationships for the i-th virtual object

$$J_{vi}=\begin{bmatrix} J_1^1 & 0 & 0 \\ 0 & J_1^2 & H_{o1}^T H_{o1} S_{o1}^T (S_{o2}^T)^{-1} H_{o2}^T H_{o2} J_{o2} \end{bmatrix} \quad (20)$$

where J_1^k is the Jacobian matrix relating the joint displacements of the arm-1 which are the part of k-th virtual arm to the k-th virtual end-effector. In this case, the rank $J_{vi1} \leq l$ depending on the location of the virtual object, and the rank $J_{vi2} \leq l$ depending on the contact types between end-effectors and the object.

On the other hand, the forward kinematic equation from the joint compliance C_j to the i-th virtual object compliance $C_{voii} \in R^{l \times l}$ can be derived in the same way as the previous section:

$$C_{vtrii}=G_{vi} C_{voii} G_{vi}^T \quad (21)$$

$$C_{vtrii}=\beta_{vi} C_j \beta_{vi}^T \quad (22)$$

2.3 Concatenated Forward Kinematics

In order to express the forward kinematics for the object and the virtual object simultaneously, we concatenate those forward kinematics:

$$dX_{tr}=GdX=\beta d\theta \quad (23)$$

$$F=G^T F_{tr} \quad (24)$$

$$\tau=\beta^T F_{tr} \quad (25)$$

where $F \in R^{nl}$ is the concatenated vector of the resultant forces/moments on the multi-object, and $F_{tr} \in R^{2(n-1)l+l_{c1}+l_{c2}}$ is the concatenated transmitted forces/moments on the multi-object from the end-effectors. n is the number of the objects whose compliance we wish to regulate. Also, $dX \in R^{nl}$ and $dX_{tr} \in R^{2(n-1)l+l_{c1}+l_{c2}}$ are the concatenated displacements of the multi-object and the concatenated transmission displacements, respectively.

The matrices $\beta \in R^{[2(n-1)l+l_{c1}+l_{c2}] \times (m_1+m_2)}$ and $G \in R^{[2(n-1)l+l_{c1}+l_{c2}] \times nl}$ are given by

$$\beta=[\beta_{v1}^T \ \cdots \ \beta_{vn-1}^T \ \beta_o^T]^T \quad (26)$$

$$G=\text{block}-\text{diag.}\,[G_{v1} \cdots G_{vn-1} \, G_o] \quad (27)$$

Consequently, the concatenated form of the forward kinematic from the joint compliance matrix, C_j, to the multi-object compliance matrix, $C \in R^{nl \times nl}$, via the transmission compliance matrix, $C_{tr} \in R^{[2(n-1)l+l_{c1}+l_{c2}] \times [2(n-1)l+l_{c1}+l_{c2}]}$, can be expressed as

$$C_{tr}=GCG^T \quad (28)$$

$$C_{tr}=\beta C_j \beta^T \quad (29)$$

where

$$C=\begin{bmatrix} C_{vo11} & C_{vo12} & \cdots & C_{vo1n} \\ C_{vo21} & C_{vo22} & \cdots & C_{vo2n} \\ & \cdots & & \\ C_{von1} & C_{von2} & \cdots & C_{vonn} \end{bmatrix} \quad (30)$$

$$C_{tr}=\begin{bmatrix} C_{vtr11} & C_{vtr12} & \cdots & C_{vtr1n} \\ C_{vtr21} & C_{vtr22} & \cdots & C_{vtr2n} \\ & \cdots & & \\ C_{vtrn1} & C_{vtrn2} & \cdots & C_{vtrnn} \end{bmatrix} \quad (31)$$

$C_{vonn} \equiv C_o \in R^{l \times l}$, $C_{vtrnn} \equiv C_{otr} \in R^{(l_{c1}+l_{c2}) \times (l_{c1}+l_{c2})}$. $C_{voij} \in R^{l \times l}$ represents the cross compliance between the i-th and j-th virtual objects and C_{vtrij} represents the cross compliance between the i-th and the j-th virtual transmission compliance.

3. Multi-Point Compliance Control for Dual-Arm Robots

Now, let's assume that the desired multi-object compliance matrix, $C^* \in R^{nl \times nl}$, is given according to the tasks. We should solve (29) for the joint compliance matrix, C_j, where the transmission compliance matrix, C_{tr}, is computed from (28).

Equation (29) may be underconstrained, overconstrained or singular depending on the matrix β. To derive a general solution of (29), we use the maximum rank decomposition of the matrix β, such that the (29) can be divided into two equations[19]:

$$C_{jb}=\beta_b C_j \beta_b^T \quad (32)$$

and

$$C_{tr}=\beta_a C_{jb} \beta_a^T \quad (33)$$

where the matrices $\beta_a \in R^{[2(n-1)l+l_{c1}+l_{c2}] \times s}$ and $\beta_b \in R^{s \times [2(n-1)l+l_{c1}+l_{c2}]}$ form the maximum rank decomposition of β: $\beta=\beta_a \beta_b$, and rank β=rank β_a=rank β_b $=s$.

We should solve (33) as the first step. In general, the exact solution C_{jb} which satisfies (33) does not exist, since the matrix β_a is a full column rank matrix. In this case, the goal is to find a matrix C_{jb} to minimize

$$G(C_{jb})=\|W(C_{tr}^*-C_{tr})W^T\| =\|W(C_{tr}^*-\beta_a C_{jb}\beta_a^T)W^T\| \quad (34)$$

where C_{tr}^* is a desired concatenated transmission compliance matrix, computed from (28) for a given desired multi-object compliance matrix C^*. $\|A\|$ stands for matrix norm defined by

$$\|A\|=[tr(A^TA)]^{0.5} \quad (35)$$

and $tr(A^TA)$ denotes trace of matrix A^TA.

Using the differential formulas about trace of matrix, we can find an optimal solution as given by

$$C_{jb}=(W\beta_a)^* WC_{tr}^* W^T\{(W\beta_a)^*\}^T \quad (36)$$

$$(W\beta_a)^*=\{(W\beta_a)^T W\beta_a\}^{-1}(W\beta_a)^T \quad (37)$$

The matrix $W \in R^{[2(n-1)l+l_{c1}+l_{c2}]\times[2(n-1)l+l_{c1}+l_{c2}]}$ is a positive definite matrix which can assign order of priority to each object according to the given task.

The second step is to solve matrix equation (32). Since the matrix β_b is of full row rank, the solution C_j which satisfy (32) always exist. The general solution is given by

$$C_j=\beta_b^+ C_{jb}(\beta_b^T)^+ + [Z-\beta_b^+\beta_b Z(\beta_b^+\beta_b)^T] \quad (38)$$

where $Z \in R^{(m_1+m_2)\times(m_1+m_2)}$ is an arbitrary constant matrix which can be utilized in the other kind of subtasks, and the superscript "+" stands for the Moore-Penrose generalized inverse.

In the proposed method, the matrix Z in (38) is set equal to zero, or we use the minimum norm solution of (32), and given by

$$C_j=\beta_b^+ C_{jb}(\beta_b^T)^+ \quad (39)$$

Then, we define the joint stiffness matrix $K_j \in R^{(m_1+m_2)\times(m_1+m_2)}$ as

$$K_j \equiv C_j^+ \quad (40)$$

Equations (36), (37), (39) and (40) give the closest object compliance to the desired one in the least squared sense for the cases which the desired compliance cannot be realized. On the other hand, when the exact solution of C_j in (29) exists, the computation of the joint compliance matrix becomes simple:

$$C_j=\beta^+ C_{tr}^*(\beta^T)^+ \quad (41)$$

because β has a full row rank.

The non-singularity of the joint stiffness matrix, K_j, can be assured like the follows: let's assume the desired multi-object compliance matrix, C^*, be positive-semidefinite matrix. Substitute (28) and (36) into (39) using C^* as C of (28), we can get

$$\begin{aligned} C_j&=\beta_b^+(W\beta_a)^{\#} WGC^*G^TW^T\{(W\beta_a)^{\#}\}^T(\beta_b^+)^T \\ &=[\beta_b^+(W\beta_a)^{\#} WG]C^*[\beta_b^+(W\beta_a)^{\#} WG]^T \end{aligned} \quad (42)$$

On the other hand, since the desired multi-object compliance matrix, C^*, is a positive-semidefinite matrix, we can write C^* in the form

$$C^*=(C^*)^{0.5}\{(C^*)^{0.5}\}^T \quad (43)$$

Substitute (43) into (42) we can get

$$\begin{aligned} C_j=&[\beta_b^+(W\beta_a)^{\#} WG(C^*)^{0.5}] \\ &\times[\beta_b^+(W\beta_a)^{\#} WG(C^*)^{0.5}]^T \end{aligned} \quad (44)$$

This means the joint compliance matrix, C_j, is a positive-semidefinite matrix[22]. Using the eigenvalues and the eigenvectors of the matrix C_j, we can decompose the matrix C_j into the form like the following

$$C_j=U\Lambda U^T \quad (45)$$

where U is the orthogonal matrix and Λ is the diagonal matrix, each component of which is the eigenvalues of the matrix C_j.

$$\Lambda=\text{diag.}[\lambda_1 \quad \lambda_2 \quad \cdots \quad \lambda_{(m_1+m_2)}] \quad (46)$$

As a result, the joint stiffness matrix, K_j, is given by

$$K_j=U\Lambda^+ U^T \quad (47)$$

where

$$\Lambda^+=\text{diag.}[\gamma_1 \quad \gamma_2 \quad \cdots \quad \gamma_{(m_1+m_2)}] \quad (48)$$

$$\gamma_i=\begin{cases}\lambda_i^{-1} & \text{if} \quad \lambda_i \neq 0 \\ 0 & \text{if} \quad \lambda_i=0\end{cases} \quad (49)$$

This secure that K_j is always non-singular.

Then we consider the stability of the realized multi-object compliance matrix, C_{real}. Using (28) and (29) we can get

$$C_{real}=G^+\beta C_j\beta^T(G^+)^T \quad (50)$$

Since C_j is a positive-semidefinite matrix, C_{real} is also a positive-semidefinite matrix. This secures the stability of the multi-object compliance control.

4. Applications to Collision Avoidance

To demonstrate the effectiveness of the proposed method, simulation experiments were performed. In the simulation experiments, the MPCC was applied to collision avoidance problem using a planar dual-arm robot as shown in **Fig. 5** ($m_1=5$, $m_2=5$, $l=3$).

The dual-arm robot is needed to perform a task

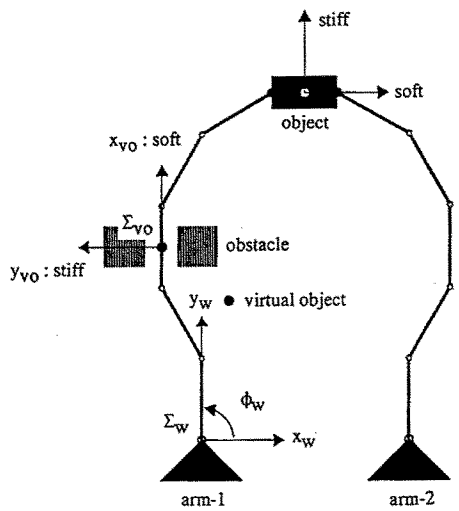

Fig. 5 A planar dual-arm robot close to an obstacle

which requires the object to be soft in the direction of x axis and the rotation (0.01 m/N and 0.1 rad/N•m, respectively) and to be stiff in the direction of y axis (0.001 m/N) in the world coordinate system.

The third link of arm-1 lies between a couple of obstacles. Therefore, a virtual object is located on the middle point of the third link of arm-1. The desired virtual object compliance is determined depending on the subtask which will be performed. In the simulation experiments, the subtask is to avoid any collision with the obstacle. The collision can be caused by the large motion of the 3rd link of the arm-1 in the direction of y_{vo} axis of the virtual object coordinate system, and the large rotation of the 3rd link of arm -1. So it is desired that the virtual object to be stiff in the direction of y_{vo} axis and its rotation (0.0005 m/N and 0.005 rad/Nm, respectively). On the other hand, since the large motion in the direction of x_{vo} axis doesn't cause the collision with the obstacle, the virtual object compliance is set to be soft in the direction of x_{vo} axis (0.01 m/N). As a result, the desired multi-object compliance matrix, $C^* \in R^{6\times 6}$ is given by

$$C^* = \text{diag.}[0.01(\text{m/N}), 0.0005(\text{m/N}), 0.005(\text{rad/Nm}), 0.01(\text{m/N}), 0.001(\text{m/N}), 0.1(\text{rad/Nm})],$$

where diag. [ ] denotes a diagonal matrix.

The simulation experiment is performed using the PD controller,

$$\tau = K_j d\theta + B_j \dot{\theta} \tag{51}$$

where $B_j \in R^{(m_1+m_2)\times(m_1+m_2)}$ is a nonsingular feedback gain matrix, and $d\theta = \theta(0) - \theta(t)$ is the joint displacements of both arms. We used the Appel method for multi-arm robots[23] and the link parameters of each arm are shown in **Table 1**. The mass and the moment of inertia of the object are 5(kg) and 0.5(kg•m^2) respectively.

Fig. 6(a) shows the initial and final postures of the dual arm under the MPCC, where the external force, $f_{ext} = [-5(\text{N}), -50(\text{N}), 0(\text{Nm})]^T$ in terms of the world coordinate system, is exerted to the center of mass of the object, and **Fig. 7**(a) shows a simulation result where we consider to control only the object compliance. The joint stiffness K_j is calculated under condi-

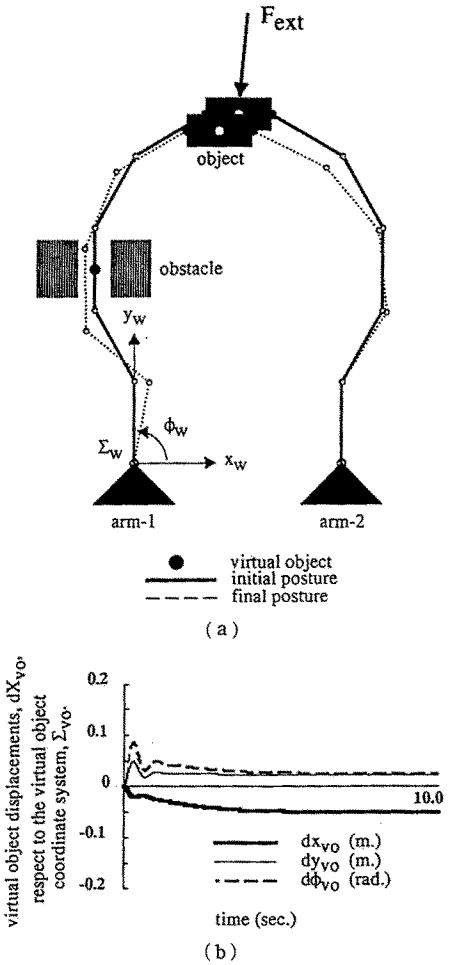

Fig. 6 Arm configuration for a disturbance force with consideration of collision avoidance using MPCC

Table 1 Link parameters of the dual-arm robot

	Arm-1 Link-i (i=1, ⋯, 6)	Arm-2 Link-i (i=1, 2, 3)
Length (m)	0.200000	0.200000
Mass (kg)	0.500000	0.500000
Center of mass (m)	0.100000	0.100000
moment of inertia (kg•m^2)	0.001500	0.001500

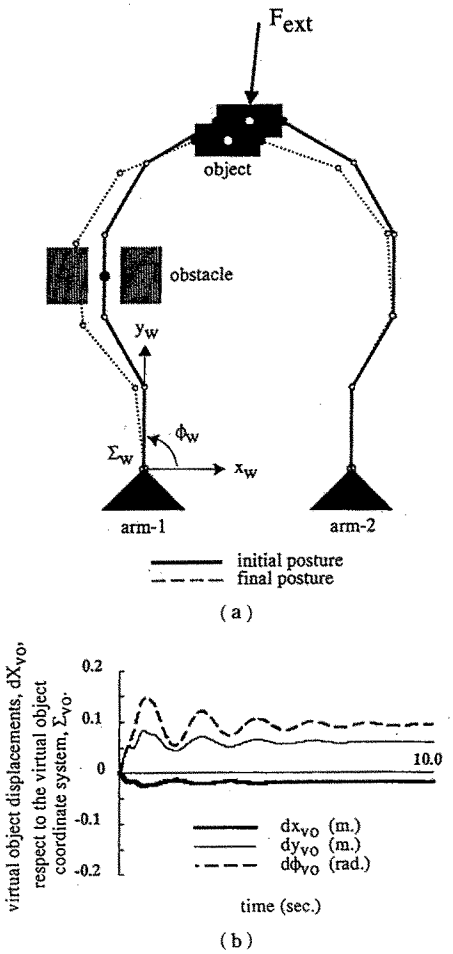

Fig. 7 Arm configuration for a disturbance force without consideration of collision avoidance

tion where the contact types between the object and both arms are the point-contact with friction ($l_{c1}=l_{c2}=2$).

On the other hand, Fig. 6(b) and Fig. 7(b) show the time history of the virtual object displacements, $dX_{vo}=[dx_{vo}\ dy_{vo}\ d\phi_{vo}]^T$, for the two kinds of the control algorithm, where dx_{vo}, dy_{vo} are the displacements in the direction of x_{vo} and y_{vo} axes of the virtual object coordinate system, respectively. $d\phi_{vo}$ is the displacement of the rotation angle of the virtual object. The displacements of the object in the steady state for the two kinds of compliance control (using the MPCC and consider to control only the object compliance) are almost the same. In terms of the virtual object, however, the effect of the MPCC appears clearly. It can be seen that the MPCC can utilize effectively the redundant joint degrees of freedom.

5. Conclusion

We have proposed the Multi-Point Compliance Control method for dual arm robots utilizing kinematic redundancy. The method was able to regulate the compliance or stiffness of several points on the dual arm's links as well as the object compliance.

In the present paper, we have concentrated on the resultant forces and moments of the object through the regulation of the joint stiffness according to a given task, for example, to restrain some external forces or to produce a desired force to generate a certain trajectory. In general, the internal compliance/stiffness which is used to stabilize the grasp and preserve the end-effector forces in the "push" direction to the object, can be controlled by the proposed method with slight change of the corresponding matrices.

The realized multi-object compliance, C_{real}, is not always equal to the desired compliance, C^*. In terms of the stability, this difference doesn't become a serious problem, because the positive-semidefiniteness of C_{real} is always hold. In term of the task purpose, however, this could be problem. This problem such as the coupling elements could be avoided by using the weighting matrix W. Unfortunately, the weighting matrix W can specify only the order of priority of the row and column of the desired multi-object compliance matrix, C^*. So, we need some improvements about the weighting function as further research.

Further research also will be directed to develop the Multi-Point Impedance Control which enable to control the impedance, not only the compliance, of several points simultaneously.

References

1) M. Uchiyama: A Unified Approach to Load Sharing, Motion Decomposing, and for Sensing of Dual Arm Robots, In: H. Miura and S. Arimoto (Eds), Robotic research: The Fifth International Symposium, Tokyo, 225/232 (1990)
2) Y. F. Zheng and J. Y. S. Luh: Joint Torques for Control of Two Coordinated Moving Robots, Proc. 1986 IEEE Int. Conf of Robotics and Automation, San Fransisco, 1375/1380 (1986)
3) V. Kumar and J. F. Gardner: Kinematics of Redun-

dantly Actuated Closed Chains, IEEE Transactions on Robotics and Automation, **RA-6**-2, 269/274 (1990)
4) C. Gosselin and J. Angeles: Singularity Analysis of Closed-Loop Kinematic Chains, IEEE Trans., **RA-6**-3, 281/290 (1990)
5) F. T. Cheng and D. E. Orin: Optimal Force Distribution in Multiple-Chain Robotic Systems, IEEE Transactions on Systems, Man, and Cybernetics, **SMC-21**-1, 13/24 (1991)
6) V. R. Kumar and K. J. Waldron: Force Distribution in Closed Kinematic Chains, IEEE J. of Robotics and Automation, **4**-6, 657/664 (1988)
7) Y. F. Zheng and J. Y. S. Luh: Optimal Load Distribution for Two Industrial Robots Handling a Single Object, Proc. 1988 IEEE Int. Conf. on Robotics and Automation, Philadelphia, 344/349 (1988)
8) T. Yoshikawa and K. Nagai: Analysis of Multi-Fingered Grasping and Manipulation, In: S. T. Venkataraman and T. Iberall (Eds), Dextrous Robot Hands, 187/208 (1990)
9) I. D. Walker and R. A. Freeman: Internal Object Loading for Multiple Cooperating Robot Manipulators, Proc. 1990 IEEE Int. Conf. on Robotics and Automation, Arizona, 606/611 (1990)
10) Y. R. Hu and A. A. Goldenberg: Dynamic Control of Multiple Coordinate Redundant Manipulator with Torque Optimization, Proc. 1990 IEEE Int. Conf. on Robotics and Automation, Ohio, 1000/1005 (1990)
11) J. Y. S. Luh and Y. F. Zheng: Computation of Input Generalized Forces for Robots with Closed Kinematic Chain Mechanisms, IEEE Journal of Robotics and Automation, **RA-1**-2, 95/103 (1985)
12) Y. Nakamura and M. Ghodoussi: Dynamic Computation of Closed-Link Robot Mechanisms with Nonredundant and Redundant Actuators, IEEE Trans., **RA-5**-3, 294/302 (1989)
13) T. Yoshikawa, Y. Yokokoji and N. Watanabe: Dynamics Analysis of Closed Link Mechanisms with Redundant Actuators, Proc. of 4th JSME Annual Conf. on Robotics and Mechatronics (ROBOMEC '92), 105/108 (1992) in Japanese.
14) M. T. Mason and J. K. Salisbury: Robot Hands and the Mechanics of Manipulation, Cambridge, MA: MIT Press (1985)
15) N. Nguyen: Constructing Force-Closure Grasps in 3-d, Proc. 1987 IEEE Int. Conf. on Robotics and Automation, 240/245 (1987)
16) M. R. Cutkosky and I. Kao: Computing and Controlling the Compliance of a Robotic Hand, IEEE Trans., **RA-5**-2, 151/165 (1989)
17) M. A. Adli, K. Nagai, K. Miyata and H. Hanafusa: Study on Internal Forces and Their Use in Compliance Control of Parallel Manipulators, Proc. of 29th SICE Annual Conference, 853/856 (1990)
18) K. Yokoi, M. Kaneko and K. Tanie: Direct Compliance Control for a Parallel Link Arm, Trans. of the JSME, **54**-505, 2131/2139 (1988) in Japanese.
19) T. Tsuji, T. Takahashi and K. Ito: Multi point Compliance Control for Redundant Manipulators, In: S. Stifter and J. Lenarcic (Eds), Advances in Robot Kinematics (1991)
20) T. Tsuji, T. Takahashi and K. Ito: Multi Point Compliance Control for Manipulators Constrained by Task Objects, Trans. of the SICE, **27**-1, 85/92 (1991) in Japanese.
21) F. T. Cheng and D. E. Orin: Efficient Formulation of Force Distribution Equations for Simple Closed-Chain, Robotic Mechanisms, IEEE Trans., **SMC-21**-1, 25/32 (1991)
22) S. Kodama and N. Suda: Matrix Theory for System Control (in Japanese). Tokyo, SICE (1978)
23) A. Jazidie, T. Tsuji, M. Nagamachi and K. Ito: Dynamic Simulation of Multi-Arm Robots Using Appel's Method, Proc. of the IFToMM-jc International Symposium on Theory of Machines and Mechanisms, 199/204 (1992)

Achmad Jazidie
(See p. 636)

Toshio Tsuji (Member)
(See p. 636)

Mitsuo Nagamachi (Member)
(See p. 636)

Koji Ito (Member)
(See p. 636)